Emerging Topics in Life Sciences (2021)
https://doi.org/10.1042/ETLS20200278

PORTLAND PRESS

Review Article

Rated-M for mesocosm: allowing the multimodal analysis of mature root systems in 3D

Tyler Dowd* Samuel McInturf* Mao Li and Christopher N. Topp

Topp Lab, Donald Danforth Plant Science Center, 975 N Warson Road, St. Louis, MO, 63124 U.S.A.

Correspondence: Christopher N. Topp (ctopp@danforthcenter.org)

A plants' water and nutrients are primarily absorbed through roots, which in a natural setting is highly dependent on the 3-dimensional configuration of the root system, collectively known as root system architecture (RSA). RSA is difficult to study due to a variety of factors, accordingly, an arsenal of methods have been developed to address the challenges of both growing root systems for imaging, and the imaging methods themselves, although there is no 'best' method as each has its own spectrum of trade-offs. Here, we describe several methods for plant growth or imaging. Then, we introduce the adaptation and integration of three complementary methods, root mesocosms, photogrammetry, and electrical resistance tomography (ERT). Mesocosms can allow for unconstrained root growth, excavation and preservation of 3-dimensional RSA, and modularity that facilitates the use of a variety of sensors. The recovered root system can be digitally reconstructed through photogrammetry, which is an inexpensive method requiring only an appropriate studio space and a digital camera. Lastly, we demonstrate how 3-dimensional water availability can be measured using ERT inside of root mesocosms.

Introduction

Increasing agricultural productivity with fewer inputs is key to combat challenges posed by an increasing global population and climate change [1,2]. Agronomically important traits (e.g. yield, nutritional content) are strongly influenced by the root systems' ability to explore the soil, compete for water and nutrients, and adapt to their local environment. Indeed, several reports show the effectiveness of targeted breeding for root traits to enhance plant survival and efficiency [3–7]. Yet, despite their fundamental importance, little is known about root biology and RSA compared with above-ground structures. Difficulties in studying roots are inherently tied to their function; being imbedded in soil keeps them hidden from observation, and iterative branching growth rapidly increases their architectural complexity. Although studying root structure and behavior is not new [8], recent technological advancements have made describing the 3-dimensional (3D) nature of root structures feasible. Despite this, currently available methods are all imperfect, and in particular, there exists a wide gap between high-information content, controlled environment experiments, and limited measurements obtainable from the field. We outline the assets and deficits of several methodologies for both plant growth and imaging, then focus on the use of mesocosms to provide a compelling balance among physiological relevance, throughput, and completeness of the RSA. Finally, we present the pairing of mesocosms with unique applications of photogrammetry to reconstruct 3D RSA, and electrical resistance tomography (ERT) to measure 3D water content dynamics, collectively producing new insights into root system structure and function.

*These authors contributed equally to this work.

Received: 20 November 2020
Revised: 12 January 2021
Accepted: 18 January 2021

Version of Record published: 8 February 2021

Growth methods for root imaging

Good root system measurements rely on the combination of plant growth, imaging, and computational analysis. Here, we focus on methods relating to plant growth and image capture; we direct readers to Atkinson et al. [9] for a review of computational methods. Each method allows the

Emerging Topics in Life Sciences (2021)
https://doi.org/10.1042/ETLS20200278

researcher to monitor specific traits which both restricts the experimental design and demands various amounts of labor, infrastructure, and know-how to conduct. To more easily parse the large number of methods, we reduced the number of techniques into coarse groups (Table 1). Each method was scored on several functional characteristics using TRUE/FALSE calls or subjective scores. The principal component analysis revealed four groups (Figure 1A) that are divided by imaging methods: 2D-optical imaging, photogrammetry, non-destructive field, and tomographic methods. Similarly, growth methods separated into three groups (Figure 1B) based primarily on where each method can be deployed: laboratory, greenhouse, or field.

State-of-the-art root phenotyping methods are a long way from achieving the ideal of comprehensive 3D root system structural and functional measurements over time in the field. Laboratory methods offer the least realistic conditions, but need little infrastructure. Methods such as 2D agarose plates (Figure 2A) have been used extensively, particularly in *Arabidopsis*, while 3D growth systems which leverage transparent media have also been used to great effect in crop species (Figure 2B) [10–12]. These approaches allow cheap, high-throughput, and non-destructive observations. Although several aspects of environmental complexity are caveated when interpreting results (e.g. 'soil' physical, chemical, and biological properties, potential root phototropic issues [13]), they have been instrumental in studies of root growth, development and environmental response. To date, they have produced the only large-scale analyses of 3D and 4D RSA [12,14–16], including recent work indicating key characteristics can persist when comparing field-grown root crowns and gel-grown plants [15].

Greenhouse methods provide more balance between the natural variance of a field and the consistency of a laboratory environment. Typically, this involves pot-grown plants (Figure 2C) which are excavated and photographed for minimal expense. While plants grown in potting mixes or reconstituted field soils provide a more realistic physiochemical environment than transparent media, disadvantages exist [17]. Increased temperature fluctuations, unrealistic water and nutrient availability, a reduced or absent soil microbiome, and physical constriction of roots may significantly affect RSA. Root mesocosms (Figure 2D), very large containers that allow

Table 1 Scoring of growth and imaging methods on functional characteristics.

		Field	Greenhouse	Laboratory	Physiological relevance	CRS at Harvest	CRS Imaged	Non-destructive	Obtain 3D info	Ease of use	Customizability	Infrastructure
Growth Methods	Trench Excavation	T	F	F	5	F		F	F	1	1	1
	3D gel	F	F	T	1	T		T	T	3	3	4
	Standard Pots	F	T	F	3	T		F	F	5	4	5
	Mesocosms	F	T	F	3	T		F	T	3	3	3
	Glass Plates	F	F	T	2	T		T	F	5	5	5
	Shovelomics	T	F	F	5	F		F	T	3	1	2
	Minirhizotrons	T	F	F	5	F		T	F	3	2	3
	Rhizotron	T	T	F	5	F		T	F	1	1	1
	Soil Cores	T	T	F	5	F		F	F	3	4	4
	2D agar plates	F	F	T	1	T		T	F	5	5	5
Imaging Methods	Photogrametry						T	F	T	3	3	4
	X-ray CT						T	T	T	2	2	2
	PET						T	T	T	1	3	2
	2D optical						T	F	F	5	5	5
	GPR						F	T	T	3	1	3
	MRI						T	T	T	1	1	2
	Minirhizotrons						F	T	F	3	2	3
	Rhizotrons						F	T	F	2	1	1
	Neutron Radiography						T	T	F	1	1	2

Binary characteristics called as TRUE (T)/FALSE (F) or scored 1–5, with higher scores being 'better' (a 'labor' score of 1 indicates an extremely labor-intensive method). Abbreviations: complete root system (CRT), computed tomography (CT), ground-penetrating radar (GPR), magnetic resistance imaging (MRI), positron emission tomography (PET).

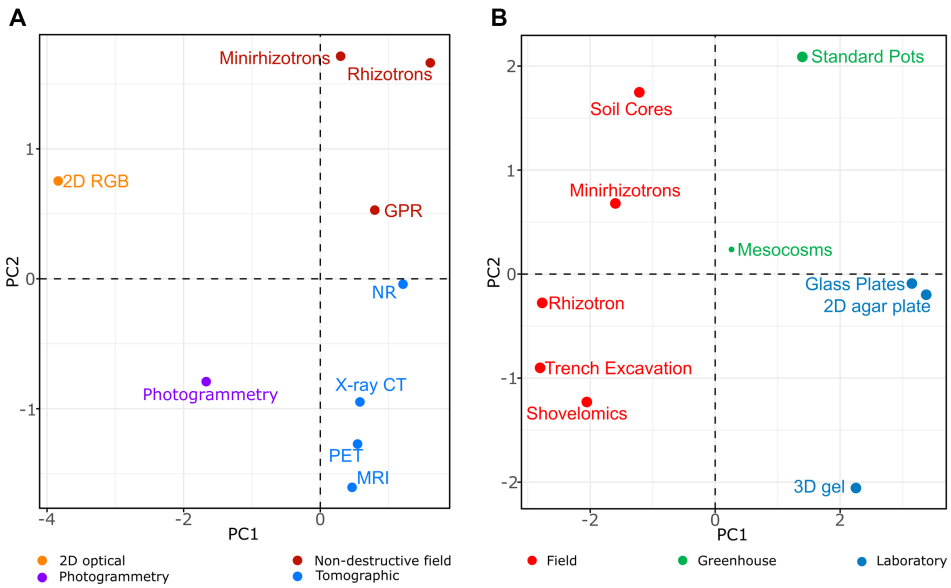

Figure 1. A course grouping of growth and imaging methods using principal components derived from Table 1.
The resulting component space describes three groups of plant growth methods and four groups of imaging methods. Resulting PCA transformations for imaging methods (**A**) where PC1 loosely describes infrastructure needed and PC2 relates the ease of use/capture of a complete root system. PCA transformations for growth methods (**B**) show a delineation of groups along PC1 relating to where the experiments can be conducted/physiological relevance and PC2 shows a mixture of covariates.

essentially unconstrained root growth in a more realistic volume of soil, offer a compelling balance between realism and control, and are discussed in detail below.

Field methods trade information content for realism [18]. The most popular method is root crown excavation with a shovel ('shovelomics' [19] (Figure 2E)). While intrinsically a small and superficial part of the overall RSA, the crown is the information-dense nexus. Root crown analysis has been effective across a diversity of research topics ranging from the effect of agricultural practices on root growth [20], drought-induced root traits [21], the identification of QTLs [22], and mutant analysis [23]. However, the desire for non-destructive measurements across the entire root system prompted the development of rhizotrons, large subterranean chambers where roots in physical contact with clear walls can be studied, requiring extensive long-term infrastructure [24–28]. Minirhizotrons, small diameter clear tubes that allow a camera to image roots touching the tube walls, were later developed and deployed *en masse* in the field. This innovation allows for multiple-timepoint sampling along a continuous depth profile [29], but considering a root system can explore dozens or hundreds of cubic feet of soil, information content is significantly limited [30]. Despite this, they have found important applications in many environments from crop fields to forests [31–33], including one of the world's most sophisticated root research facilities [34]. Soil cores offer a similar estimation of RSA as minirhizotrons, and although destructive, the recovered root and soil samples can be further analyzed [35–37]. Trench excavations and soil monoliths date back to at least the early 1900s [38–40] (Figure 2F) and offer the most complete data of any field method, but at an incredible infrastructure and labor cost. While modern incarnations have incorporated some basic image analysis [23,41], data acquired from trenches has been largely descriptive with coarse quantification of typically only a cross section of the actual 3D RSA.

Imaging methods for root systems

Our classification system identified four general groups of imaging methods (Figure 1). The imaging environment, sample preparation, and processed data which these methods capture is shown in Figure 3.

2D-optical imaging with a digital camera or flatbed scanner provides the most versatile and least expensive imaging method (Figure 3A–C). Although the 3rd dimension is sacrificed, entire root systems can be measured

Emerging Topics in Life Sciences (2021)
https://doi.org/10.1042/ETLS20200278

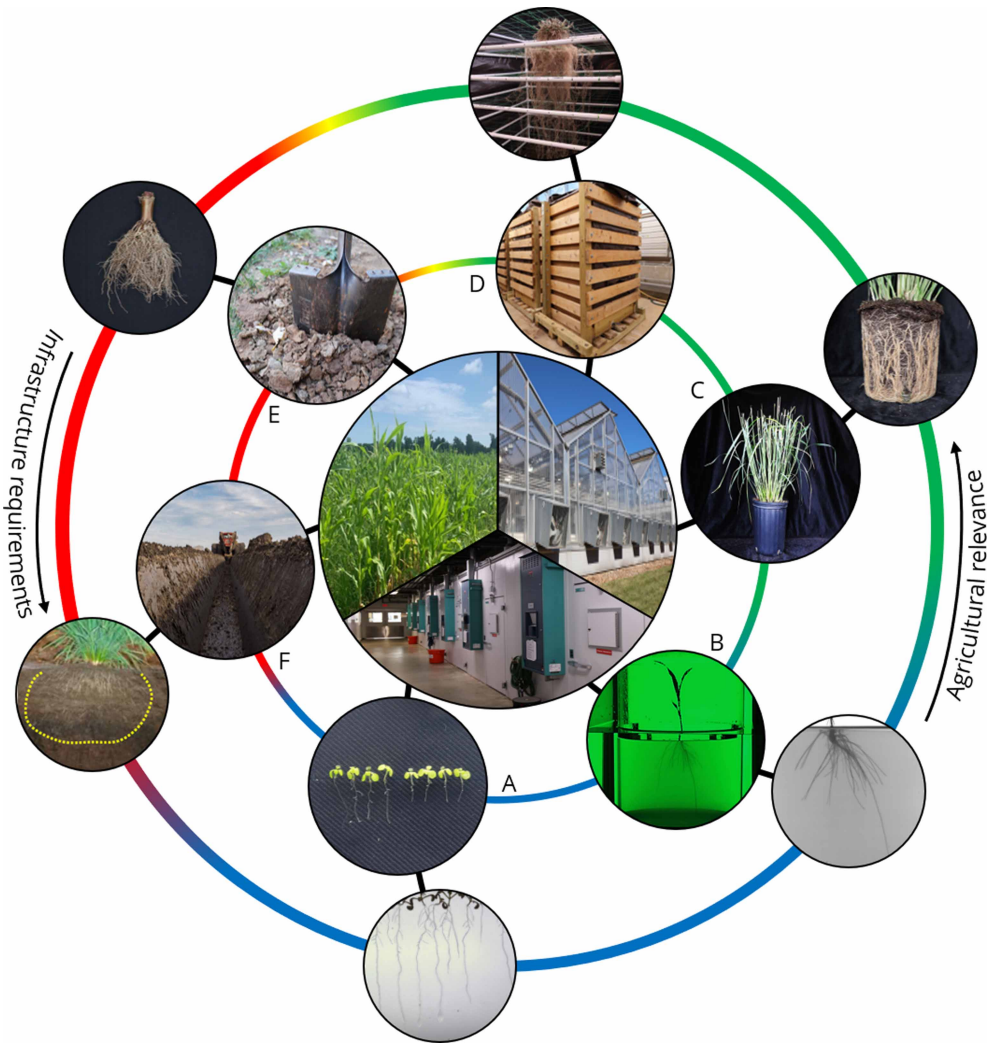

Figure 2. Visual representation of the growth methods.

Inner ring shows the environment where the plants are grown/harvested while the outer ring shows the roots obtained by the method to be analyzed. Infrastructure requirements increase counter clockwise within each setting (laboratory, greenhouse, field); likewise agricultural relevance increases from (**A**) to (**F**). (**A**) *Arabidopsis thaliana* grown on agarose plates, (**B**) *Zea maize* grown in a gum agar system, (**C**) *Panicum virgatum* (switchgrass) grown in a greenhouse pot, (**D**) *Panicum virgatum* grown in a mesocosm, (**E**) *Zea mays* excavated for shovelomics (**F**) trench dug for root examination of Oryza sativa, the yellow dotted line shows the extent of root elongation [83].

either *in situ* or excavated, intact or in pieces, depending on the approach. Many algorithms and software packages have been devised to extract complex features and traits from still images [39]. Programs such as DIRT [42,43], archiDART [44], EZ-Root-VIS [45], GiA Roots [46], WinRHIZO (Regent Instrument Inc., Ville de Québec, QC Canada), and RhizoVision [47] provide a means to measure of a variety of traits of interest; such as root lengths, diameter classes, volumes, and surface areas of individual roots or entire root systems of many species, for example, *Zea mays* [48].

Tomographic methods, which employ a series of 2-dimensional slices to generate a 3D volume, include X-ray tomography (XRT), magnetic resonance imaging (MRI), and positron emission tomography (PET) (Figure 3J–R). They provide non-destructive, high-resolution data of external and internal structures or the movement of small molecules through a root system. Adopted from medical and industrial imaging facilities, they typically require expensive equipment, highly trained users, and a dedicated space. While information content is high, including 3D and 4D growth and physiological dynamics, they are limited to relatively small-

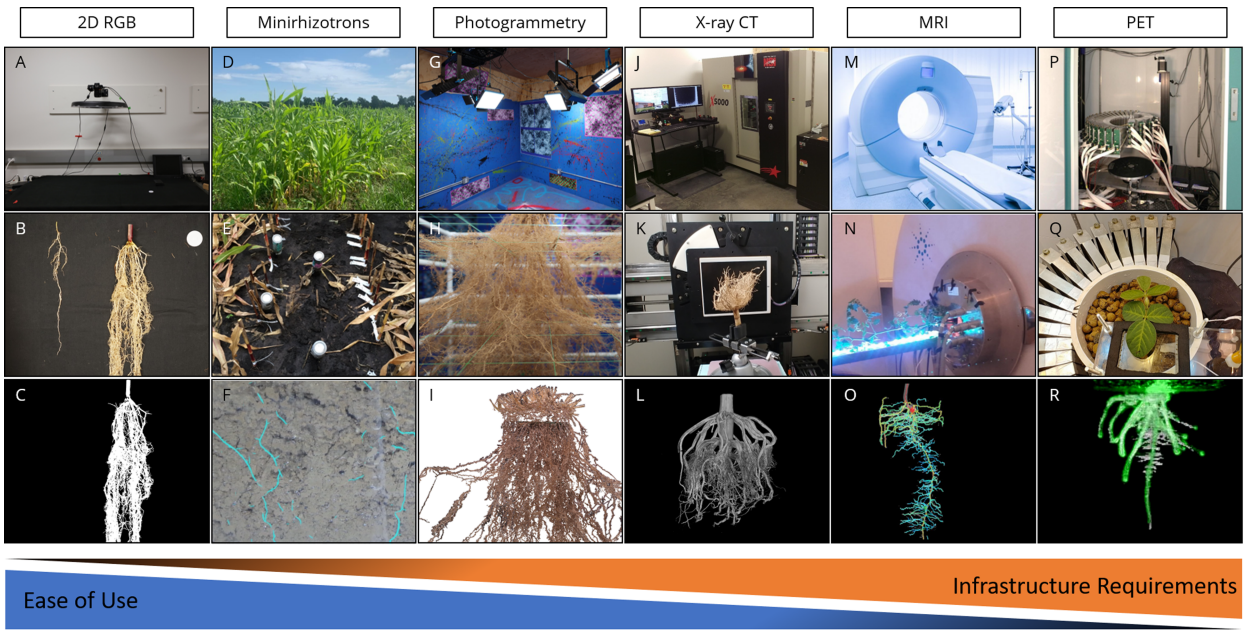

Figure 3. Example depictions for several of the imaging methods.

Top row shows apparatus/location where the method is deployed, middle row shows examples of samples being imaged, bottom row shows used/reconstructed data. (**A**–**C**) 2D-optical imaging station, W22 *Zea mays* root system, and processed image via DIRT software. (**D**–**F**) Minirhizotron system deployed in the field showing roots of *Cichorium intybus L.* pressed against the tube surface and processed using RootPainter [81]. (**G**–**I**) A Photogrammetry studio and suspended WBC3 switchgrass root system and subsequent point cloud reconstruction via Pix4D. (**J**–**L**) X-ray tomography suite reconstructing field excavated maize root crowns. (**M**) a modern MRI studio, typically used for human subjects, a modified MR system for analyzing plant samples (**N**) [83], resulting data map of root diameters (**O**) [84], (**P**) PET imaging system imaging carbon flux to the roots of (**Q**) *Glycine* max grown in expanded clay, panel (**R**) shows PET/CT overlay of a *Zea mays* seedling.

diameter pots, are moderately low throughput, and require extensive image processing and analysis. Nonetheless, advancements have been made recently in developing these tools for impactful plant science. Although differences in equipment and experimental parameters can vary, typically XRT has finer resolution (10s–100s μm) with lower penetration of the growth media, while MRI has lower resolution (100s–1000s μm) but accommodates larger pots [49]. Recently, advances have been made utilizing PET in conjunction with XRT or MRI to pair structure with function (Figure 3R). The movement of these radioisotopes can be detected in real-time at high-resolution (1–5 mm) and provide extraordinary power to the study water and nutrient uptake [50–52]. Another emerging technology is the use of neutron radiography (NR) to assess root structure and function. This has been used to not only reconstruct pot-grown root systems but also can provide high-resolution (10s–100s μm) 3D information of water distribution in the rhizosphere [53], as well as assess the individual water uptake capacity of specific roots in a single system [54]. Furthermore, NR has been paired with fluorescent dyes to image changes in rhizosphere oxygen content [55], and is hypothesized to be capable of assessing the dynamics of a variety of environmental factors.

The group 'non-destructive field imaging' includes two methods: minirhizotrons and ground-penetrating radar (GPR) (Figure 3D–F). Minirhizotrons capture 2D-optical images from cameras in buried tubes and are the only method, aside from dedicated rhizotron facilities, for observing time-course root traits in a field setting. GPR systems emit and detect radio waves that can identify underground roots [56]. While GPR is capable of surveying large plots, it is sharply limited by the minimum detectable root size (0.5+ cm) [57]. Hence GPR is an effective in forestry, but has limited applications for row crops without significant increases in resolution.

The methods presented here represent an array of creative solutions to the study of RSA. Advances in the applications of medical imaging technology to plant science have given us the ability to quantify detailed growth, morphology, and physiological processes at multiple scales. However, we thus far cannot capture the structure of mature root systems that reflect their *in situ* 3D configuration, nor can we easily collect

Emerging Topics in Life Sciences (2021)
https://doi.org/10.1042/ETLS20200278

concomitant dynamic environmental or physiological information in structures larger than a simple pot. In the following sections, we present the use of low-cost cameras and large root growth boxes (mesocosms) to generate 3D reconstructions of entire, unconstrained RSAs (Figure 3G–I), in combination with real-time sensor arrays.

Modern mesocosms for modern root studies

Mesocosms, medium-scale experimental systems that are meant to span the gap between the laboratory and field, offer aspects of both environmental control and realism. An old idea that spans many disciplines of biology, these systems vary widely even within the plant and ecological sciences [58–63]. Our concern was to preserve the 3D RSA of *freely grown* and *mature* crops, growing in physiologically relevant conditions, at a scale where multidimensional environmental gradients can effectively be measured and modeled (Figure 4). The mesocosms presented here are large growth containers (45 ft^3 [1.3 m^3]) which are scalable and allow for completely, or near-unrestricted root growth of full-size crop plants (Figure 4A). Within the container, several tiers of thin wire form a grid scaffold, and at harvest the root system is carefully excavated, preserving the 3D architecture. Multiple plant species and varieties have been grown and subsequently imaged via photogrammetry (discussed below), including switchgrass ecotypes VS16 and WBC3 (Figure 4B), from which 3D traits have been extracted (Figure 4C). The internal scaffold can also be used to isolate distinct spatial regions. Allowing for subsampling the system to match other phenotyping methods, such as isolating root crowns

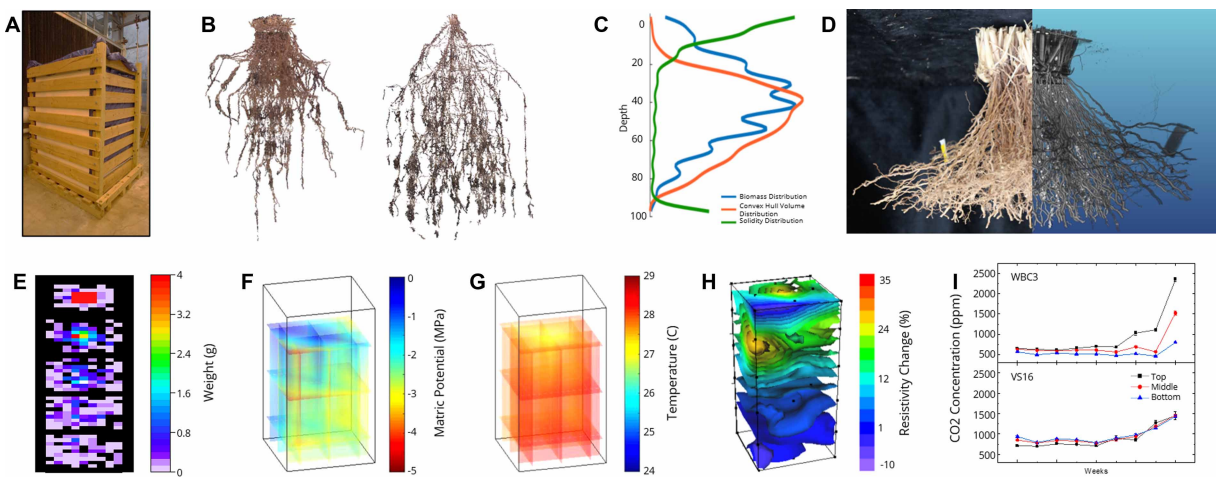

Figure 4. Root system mesocosms allow for both 3D reconstruction and 3D sensor data.

(**A**) Large format mesocosm with a growth media volume of 45 ft^3 [1.3 m^3], 3 × 3×5 ft [0.9 × 0.9 × 1.5 m] (3.5′ × 4.5′ × 6′ exterior structure), used to grow full size root systems under a variety of conditions. (**B**) Point clouds of *Panicum virgatum* varieties VS16 (left) and WBC3 (right) grown in mesocosms for 14 weeks. (**C**) 3D architecture traits extracted from switchgrass point clouds, including biomass, convex hull volume, and solidity with depth. Trait extraction was facilitated by assessing the voxel distribution in 3D space in MATLAB R2017a (The MathWorks, Inc. Massachusetts, United States). Biomass distribution is a function of voxel number by depth, convex hull is the extent of the 3D space voxels occur, and solidity is a measurement of biomass/convex hull. (**D**) 2D-optical image and associated XRT reconstruction of a WBC3 switchgrass root crown. XRT scans were conducted on a North Star Imaging X5000 X-ray Computed Tomography system. Projections were reconstructed into single 3D volumes using NSI efX-ct software [15]. (**E**) Ground truth for root biomass collected from each 'cell' within the internal mesocosm frame for the top 2.5 ft of growth volume. Each cell consisted of a 4″ × 4″ × 6″ sub section of the growth volume. The root system was manually dissected from bottom up and each cell was individually weighed. Heat maps of biomass were constructed for each 6-inch z-layer. (**F**–**H**) Reconstructions of 3D water potential, temperature, and electrical resistance fluxes. 3D visualization of temperature and matric potential were generated by interpolation of data gathered by TEROS 21 (METER Group, Inc. Washington, United States) sensor arrays inside the mesocosm growth volume. A Delaunay triangulation method based linear interpolation was conducted in MATLAB R2017a using the function griddatan(). ERT measurements and analysis were made using a SuperSting R8, an array of buried electrodes, and AGI EarthImager 3D software (Advanced Geosciences Inc. Texas, United States). (**I**) CO_2 measurements of two switchgrass varieties at three depths within the mesocosm over the course of 9 weeks, top (1.25 ft [0.38 m] deep), middle (2.75 ft [0.84 m] deep), and bottom (4.25 ft [1.30 m] deep). CO_2 measurements were conducted using a G2201-i isotopic analyzer and a 16-port distribution manifold (Picarro, Inc. California, United States).

analogous to shovelomics samples. Figure 4E shows biomass collected in each cuboid at five z-levels providing a ground truth for computational approaches.

While multiple sensor probes can be deployed in any pot, the scale of traditional containers makes this additional data redundant. In a mesocosm, probes placed at multiple depths allow for measurements of biologically meaningful gradients in media matric potential, temperature, electrical resistance, CO_2, *et cetera* (Figure 4F–I). Currently these gradients can be compared with the recovered root system to form *post hoc* prediction of root activity, with an aim to utilize one or more combination of sensor arrays to detect root activity *in vivo*.

Although the root mesocosm system is a powerful tool which does not require singularly expensive components, it does come at the expense of labor and space. A single mesocosm of the size described here costs a few hundred USD in lumber, nuts/bolts. Dedicated spaces and tools (pallet jacks) are important to store and handle the volume of media used in a mesocosms suite, and the physical labor required to un/load them is significant. Moreover, their weight requires reinforced concrete floors and substantial space to deploy, considering only a dozen mesocosms can cover a small (~700 ft^2) greenhouse. This is non-trivial, as establishing enough replicates to overcome the biological variance found in RSA may limit avenues of experimentation. As such, mesocosms are most useful as an in-between step from laboratory/greenhouse discovery to field testing, determining if juvenile traits continue onto maturity. If maintained, performance can be evaluated in the field. Furthermore, many other crops, such as fruits/vegetables or smaller cover crops, such as pennycress, could utilize significantly smaller units based on their RSA; potentially small enough to run large-sample size experiments in a greenhouse. Finally generating a point cloud that can be reconstructed though photogrammetry requires a dedicated studio which has multiple considerations in its size, location, and layout.

Leveraging photogrammetry for root system reconstruction

Photogrammetry, the use of 2D-photographs to create geometric reconstructions of 3D objects, is a powerful imaging methodology because it is decoupled from specific experimental environments, finding applications in the laboratory (gel imaging), greenhouse (mesocosms), and in the field (shovelomics). In a photogrammetry studio (Figure 5A) the sample is positioned to minimize shadows and allow for 360° imaging (Figure 5B). Images are collected from around the subject (Figure 5C) and the individual images are used to form a reconstructed 3D point cloud (Figure 5D), after which the background is removed via image processing to isolate the sample (Figure 5E). This point cloud is then cleaned semi-automatically (Figure 5F) and skeletonized into a network system (Figure 5G). This workflow from 2D projections to a 3D model is similar to other tomography-family methods. A key difference is the sensor moves freely relative to the sample during photogrammetry, rather than rotating around a fixed axis. As such, there are spatial restrictions (sample dimensions) to what can be imaged. During reconstruction individual voxels are mapped to a 3D space to produce a point cloud, then a surface mesh and/or a skeleton is derived to generate the defined root system object. At this point, many of the postprocessing algorithms initially designed for tomographic methods such as XRT [15,64] and MRI can be used as the 3D representations are interoperable. Additionally, this opens up other avenues of analysis, such as persistent homology to assess holistic growth patterns [65].

Projections from methods such as XRT allow the resolution of internal features, since X-rays penetrate the sample. Conversely, photogrammetry captures reflected light, so any internal structure, or any feature outside of line-of-sight cannot be simply reconstructed, as occurs in dense root crowns. Photogrammetry also relies on significant computational power and dedicated reconstruction software (e.g. Pix4D). Despite these requirements, photogrammetry offers the lowest financial barrier, a few hundred dollars for a standard digital camera and $4990 for a perpetual Pix4D license, the greatest sample-type flexibility, and when paired with mesocosms provide a novel view of RSA.

Electrical resistance tomography to map 4D water availability

ERT is a technique developed to observe subterranean structures and processes through electrical pulses emitted from electrodes [66]. Probes are laid in a line or encircling an object to obtain data on a specific transect, such as CO_2 fluxes deep in underground pools [67], monitoring the rate of water infiltration into concrete [68], or to determine different geological layers across a survey site [69]. However, if electrodes are buried and arrayed in a grid, then 3D resistivity measurements can also be obtained [70] and have been used to observe

Emerging Topics in Life Sciences (2021)
https://doi.org/10.1042/ETLS20200278

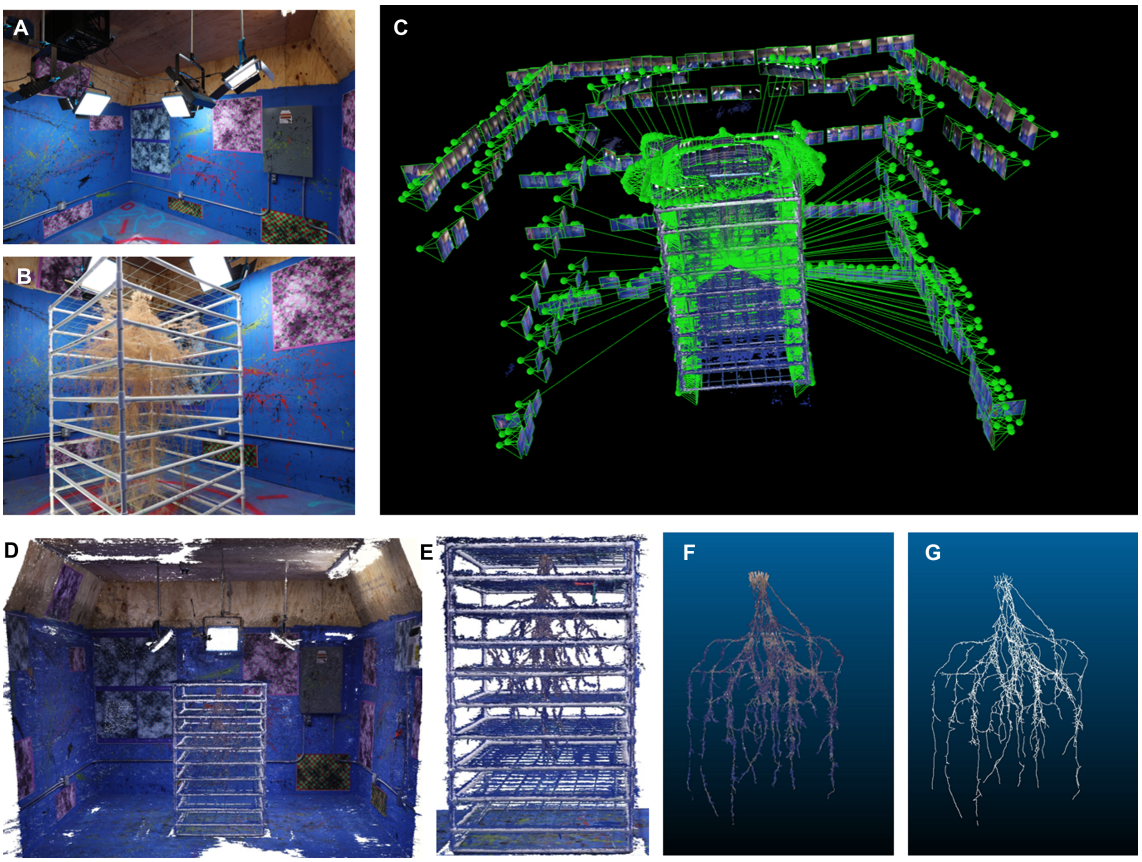

Figure 5. Steps in a photogrammetry workflow.

(**A**) Photogrammetry studio with strong, consistent illumination and non-repeating backgrounds on the walls for camera alignment. (**B**) Mesocosm grown switchgrass sample positioned for imaging. (**C**) Background subtracted reconstruction of (**B**) where each green orb indicates the location of a captured and aligned 2D-optical image. Images were captured using a Canon 50D. Green lines indicate which of the 2D images are using the selected identification point for alignment. (**D**) Complete reconstruction of the photogrammetry studio. Data are processed from a noisy (**E**) to a clean (**F**) point cloud, which is finally skeletonized for analysis (**G**). All photogrammetric analysis was conducted using Pix4D mapper software (Pix4D S.A. Prilly, Switzerland), and point cloud cleaning and skeletonization were conducted in CloudCompare V2. 10.2 and MATLAB R2017a, respectively.

the dynamics of sub-surface gas–liquid mixing [71], CO_2 fluxes [72], and high-resolution variances in soil water content [73].

ERT has been used in multiple studies to assess the spatial distribution of electrical resistance influenced by water uptake correlated to root biomass [73–75]. Other interesting uses have been found, such as assessing the distribution of tree roots in woodlands [76], identifying preferred pathways of underground water flow, and providing information on relative levels of water uptake across a single tree's root system [77]. On the larger scale, ERT has been used to assess metrics such as water levels and soil types across field plots [73,78–80].

We used an ERT probe array (Figure 6A,B) to monitor electrical resistivity in a switchgrass mesocosm over the course of 42 days. Comparing 28, 38, and 42 days to 14 days after transplant allows us to visualize water-poor shells which are co-localized to known root masses (Figure 6C). While this has only allowed for estimations of gross root location, further refinement of probe layouts and densities could be used to develop real-time maps of root activity. Furthermore, if ERT sensor co-ordinates are paired with the internal co-ordinate system of the mesocosms the resultant 3D point clouds can be aligned with 4D resistivity fluxes. If expanded this could be used to effectively monitor fluxes under many experimental conditions; such as plant-to-plant below-ground competition, or relative water uptake of various roots of a single system. If scaled up it could be possible to holistically monitor the 3D water flux under entire field plots, pinpointing locations of specific

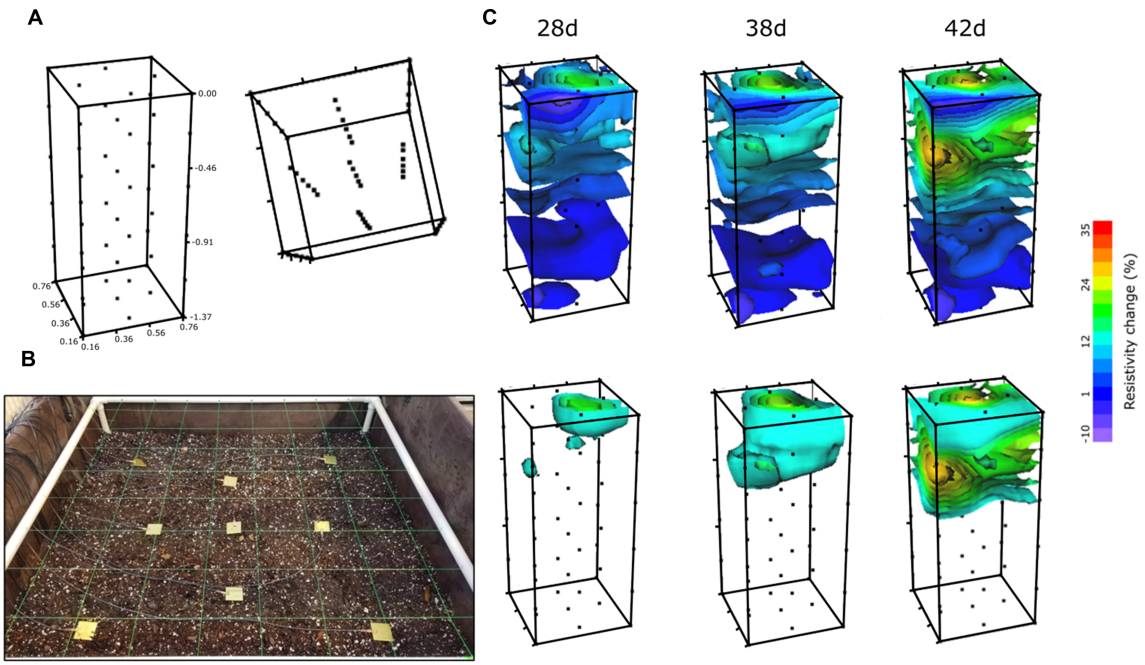

Figure 6. Example electrical resistance tomography data.

(**A**) The mesocosm was outfitted with six layers of nine ERT sensors to detect resistivity changes through the entire column, scale is in meters. (**B**) Layout of the probes, the boundary box in (**A**) are defined by the four corner sensors. (**C**) Time course comparisons of resistivity, comparing each day to 14 d after the transplantation of a young WBC3 switchgrass plant. The warm tone contour shells show areas of higher resistivity, relating to dryer regions in the column, e.g. areas of active water uptake. The lower three images show the resistivity change data thresholded to only show changes over 10 percent. ERT measurements and analysis were made using a SuperSting R8, an array of buried electrodes, and AGI EarthImager 3D software.

changes in water dynamics in real-time, allowing for a targeted approach to water management and true measurements of below-ground physiological functions.

Conclusion

The study of root systems has progressed from marveling at the capacity of roots to penetrate nutrient-poor soils, seeking out nutrient-dense patches, to the generation of VR-ready root systems. While the heart of the problem in studying roots has not changed (they are underground, complex, and dynamic structures), the number and scope of solutions has grown substantially. Here, we summarized many tried-and-true methods such as trenches and agar plates to the most technologically advanced tomographic methods. While all these methods have clear strengths and weaknesses, none are capable of quantifying the 3D root structure of whole root systems grown unconstrained the way mesocosms paired with photogrammetry can. They can be scaled up to larger containers to study multi-plant root system interactions, and co-ordinate with above-ground phenotyping tools, while being relatively inexpensive and straightforward to construct. Furthermore, pairings with existing and developmental-stage sensors can provide an additional dimension of dynamic chemical flux. The necessity to improve our understanding of desired root traits cannot be understated with the threat of climate change on our doorstep. The methods outlined here provide a methodological backbone for researchers as we work towards developing lines which more efficiently harvest water and nutrients at both shallow and deep soil depths.

Competing Interests

The authors declare that there are no competing interests associated with the manuscript.

Author Contributions

T.D. conducted experiments. T.D., S.M., and C.N.T. wrote the manuscript. M.L. analyzed the matric potential/temperature data.

Acknowledgements

We would like to thank Dr. Bradly Carr for instruction and assistance with ERT, Michael Schoenewies for expert advice on photogrammetry, the authors of [81,82] for use of Figure 3F,N under the CC-BY creative commons license, and the authors of [83] for their personal permission to reproduce image 2F under the CC-BY-NC-ND license. Finally, Plant Physiology for the reuse of the image 3O from [84]. Images 2F and 3M were obtained via Shutterstock. This material is based upon work supported by the Department of Energy under Award number: DE-AR0000820 and the National Science Foundation under Award number: IOS-1638507.

Abbreviations

ERT, electrical resistance tomography; GPR, ground-penetrating radar; NR, neutron radiography; PET, positron emission tomography; RSA, system architecture; XRT, X-ray tomography.

References

1 Campbell, B.M., Vermeulen, S.J., Aggarwal, P.K., Corner-dolloff, C., Girvetz, E., Maria, A. et al. (2016) Reducing risks to food security from climate change. *Glob Food Sec.* **11**, 34–43 https://doi.org/10.1016/j.gfs.2016.06.002

2 Springmann, M., Clark, M., Mason-D'Croz, D., Wiebe, K., Leon Bodirsky, B., Lassaletta, L. et al. (2018) Options for keeping the food system within environmental limits. *Nature* **562**, 519–525 https://doi.org/10.1038/s41586-018-0594-0

3 Gahoonia, T.S. and Nielsen, N.E. (2004) Root traits as tools for creating phosphorus efficient crop varieties. *Plant Soil* **260**, 47–57 https://doi.org/10.1023/B:PLSO.0000030168.53340.bc

4 Nguyen, H.T., Babu, R.C. and Blum, A. (1997) Breeding for drought resistance in rice: physiology and molecular genetics considerations. *Crop Sci.* **37**, 1426–1434 https://doi.org/10.2135/cropsci1997.0011183X003700050002x

5 Sandhu, N., Anitha Raman, K., Torres, R.O., Audebert, A., Dardou, A., Kumar, A. et al. (2016) Rice root architectural plasticity traits and genetic regions for adaptability to variable cultivation and stress conditions. *Plant Physiol.* **171**, 2562–2576 https://doi.org/10.1104/pp.16.00705

6 Swamy, B.M. and Kumar, A. (2013) Genomics-based precision breeding approaches to improve drought tolerance in rice. *Biotechnol. Adv.* **31**, 1308–1318 https://doi.org/10.1016/j.biotechadv.2013.05.004

7 Zhan, A. and Lynch, J.P. (2015) Reduced frequency of lateral root branching improves N capture from low-N soils in maize. *J. Exp. Bot.* **66**, 2055–2065 https://doi.org/10.1093/jxb/erv007

8 Knight, T.A. (1811) On the causes which influence the direction of the growth of roots. *Philos. Trans. R. Soc. Lond.* **101**, 209–219 https://doi.org/10.1098/rstl.1811.0013

9 Atkinson, J.A., Pound, M.P., Bennett, M.J. and Wells, D.M. (2019) Uncovering the hidden half of plants using new advances in root phenotyping. *Curr. Opin. Biotechnol.* **55**, 1–8 https://doi.org/10.1016/j.copbio.2018.06.002

10 Downie, H., Holden, N., Otten, W., Spiers, A.J., Valentine, T.A. and Dupuy, L.X. (2012) Transparent soil for imaging the rhizosphere. *PLoS One* **7**, 1–6 https://doi.org/10.1371/journal.pone.0044276

11 Ma, L., Shi, Y., Siemianowski, O., Yuan, B., Egner, T.K., Mirnezami, S.V. et al. (2019) Hydrogel-based transparent soils for root phenotyping in vivo. *Proc. Natl. Acad. Sci. U.S.A.* **166**, 11063–11068 https://doi.org/10.1073/pnas.1820334116

12 Topp, C.N., Iyer-Pascuzzi, A.S., Anderson, J.T., Lee, C.-R., Zurek, P.R., Symonova, O. et al. (2013) 3D phenotyping and quantitative trait locus mapping identify core regions of the rice genome controlling root architecture. *Proc. Natl. Acad. Sci. U.S.A.* **110**, E1695–E1704 https://doi.org/10.1073/pnas.1304354110

13 Van Gelderen, K., Kang, C. and Pierik, R. (2018) Light signaling, root development, and plasticity. *Plant Physiol.* **176**, 1049–1060 https://doi.org/10.1104/pp.17.01079

14 Hufnagel, B., de Sousa, S.M., Assis, L., Guimaraes, C.T., Leiser, W., Azevedo, G.C. et al. (2014) Duplicate and conquer: multiple homologs of PHOSPHORUS-STARVATION TOLERANCE1 enhance phosphorus acquisition and sorghum performance on low-phosphorus soils. *Plant Physiol.* **166**, 659–677 https://doi.org/10.1104/pp.114.243949

15 Jiang, N., Floro, E., Bray, A.L., Laws, B., Duncan, K.E. and Topp, C.N. (2019) Three-dimensional time-lapse analysis reveals multiscale relationships in maize root systems with contrasting architectures. *Plant Cell* **31**, 1708–1722 https://doi.org/10.1105/tpc.19.00015

16 Wedger, M.J., Topp, C.N. and Olsen, K.M. (2019) Convergent evolution of root system architecture in two independently evolved lineages of weedy rice. *New Phytol.* **223**, 1031–1042 https://doi.org/10.1111/nph.15791

17 Passioura, J.B. (2006) The perils of pot experiments. *Funct. Plant Biol.* **33**, 1075–1079 https://doi.org/10.1071/FP06223

18 Bray, A.L. and Topp, C.N. (2018) The quantitative genetic control of root architecture in maize. *Plant Cell Physiol.* **59**, 1919–1930. https://doi.org/10.1093/pcp/pcy141

19 Trachsel, S., Kaeppler, S.M., Brown, K.M. and Lynch, J.P. (2011) Shovelomics: High throughput phenotyping of maize (*Zea mays L.*) root architecture in the field. *Plant Soil* **341**, 75–87 https://doi.org/10.1007/s11104-010-0623-8

20 Zhan, A., Liu, J., Yue, S., Chen, X., Li, S. and Bucksch, A. (2019) Architectural and anatomical responses of maize roots to agronomic practices in a semi-arid environment. *J. Plant Nutr. Soil Sci.* **182**, 751–762 https://doi.org/10.1002/jpln.201800560

21 Kengkanna, J., Jakaew, P., Amawan, S., Busener, N., Bucksch, A. and Saengwilai, P. (2019) Phenotypic variation of cassava root traits and their responses to drought. *Appl. Plant Sci.* **7**, 1–14 https://doi.org/10.1002/aps3.1238

22 Zheng, Z., Hey, S., Jubery, T., Liu, H., Yang, Y., Coffey, L. et al. (2020) Shared genetic control of root system architecture between *Zea mays* and sorghum bicolor1[OPEN]. *Plant Physiol.* **182**, 977–991 https://doi.org/10.1104/pp.19.00752

23 Kitomi, Y., Hanzawa, E., Kuya, N., Inoue, H., Hara, N., Kawai, S. et al. (2020) Root angle modifications by the DRO1 homolog improve rice yields in saline paddy fields. *Proc. Natl. Acad. Sci. U.S.A.* **117**, 21242–21250 https://doi.org/10.1073/pnas.2005911117

24 Atkinson, D. (1985) Spatial and temporal aspects of root distribution as indicated by the use of a root observation laboratory. *Spec. Publ. Br. Ecol. Soc.* 43–65 https://pascal-francis.inist.fr/vibad/index.php?action=getRecordDetail&idt=9239868

25 Head, G.C. (1966) Estimating seasonal changes in the quantity of white unsuberized root on fruit trees. *J. Hortic. Sci.* **41**, 197–206 https://doi.org/10.1080/00221589.1966.11514168
26 Head, G.C. (1967) Effects of seasonal changes in shoot growth on the amount of unsuberized root on apple and plum trees. *J. Hortic. Sci.* **42**, 169–180 https://doi.org/10.1080/00221589.1967.11514205
27 Rutherford, M.C. and Curran, B. (1981) A root observation chamber for replicated use in a natural plant community. *Plant Soil* **63**, 123–129 https://doi.org/10.1007/BF02374591
28 Taylor, H.M. (1969) The rhizotron at auburn, alabama - a plant root observation laboratory. *Auburn Univ. Agric. Exp. Stn.* **171**, 1–9 http://aurora.auburn.edu/bitstream/handle/11200/1968/1169CIRC.pdf
29 Johnson, M.G., Tingey, D.T., Phillips, D.L. and Storm, M.J. (2001) Advancing fine root research with minirhizotrons. *Environ. Exp. Bot.* **45**, 263–289 https://doi.org/10.1016/S0098-8472(01)00077-6
30 Taylor, H.M., Upchurch, D.R. and McMichael, B.L. (1990) Applications and limitations of rhizotrons and minirhizotrons for root studies. *Plant Soil* **129**, 29–35 https://doi.org/10.1007/BF00011688
31 Bragg, P.L., Govi, G. and Cannell, R.Q. (1983) A comparison of methods, including angled and vertical minirhizotrons, for studying root growth and distribution in a spring oat crop. *Plant Soil* **73**, 435–440 https://doi.org/10.1007/BF02184322
32 Graefe, S., Hertel, D. and Leuschner, C. (2008) Estimating fine root turnover in tropical forests along an elevational transect using minirhizotrons. *Biotropica* **40**, 536–542 https://doi.org/10.1111/j.1744-7429.2008.00419.x
33 Hendrick, R.L. and Pregitzer, K.S. (1996) Applications of minirhizotrons to understand root function in forests and other natural ecosystems. *Plant Soil* **185**, 293–304 https://doi.org/10.1007/BF02257535
34 Svane, S.F., Jensen, C.S. and Thorup-Kristensen, K. (2019) Construction of a large-scale semi-field facility to study genotypic differences in deep root growth and resources acquisition. *Plant Methods* **15**, 1–16 https://doi.org/10.1186/s13007-019-0409-9
35 Bloodworth, M.E., Burleson, C.A. and Cowley, W.R. (1958) Root distribution of some irrigated crops using undisrupted soil cores 1. *Agron. J.* **50**, 317–320 https://doi.org/10.2134/agronj1958.00021962005000060009x
36 Jakobsenl, I., Gazey, C. and Abbott, L.K. (2001) Phosphate transport by communities o mycorrhizal fungi in intact soil cores. *New Phytol.* **149**, 95–103 https://doi.org/10.1046/j.1469-8137.2001.00006.x
37 Wasson, A.P., Rebetzke, G.J., Kirkegaard, J.A., Christopher, J., Richards, R.A. and Watt, M. (2014) Soil coring at multiple field environments can directly quantify variation in deep root traits to select wheat genotypes for breeding. *J. Exp. Bot.* **65**, 6231–6249 https://doi.org/10.1093/jxb/eru250
38 Böhm, W. (1979) Root parameters and their measurement. In *Methods of Studying Root Systems* (Billings, W.D., Golley, F., Lange, O..L. and Olson, J. S., eds), pp. 125–138, Springer, Berlin Springer Science & Business Media
39 Weaver, J.E. (1915) A study of the root-systems of prairie plants of southeastern Washington. *Plant World* **18**, 227–248
40 Weaver, J.E. (1958) Classification of root systems of forbs of grassland and a consideration of their significance. *Ecology* **39**, 393–401 https://doi.org/10.2307/1931749
41 Teramoto, S., Kitomi, Y., Nishijima, R., Takayasu, S., Maruyama, N. and Uga, Y. (2019) Backhoe-assisted monolith method for plant root phenotyping under upland conditions. *Breed Sci.* **513**, 508–513 https://doi.org/10.1270/jsbbs.19019
42 Das, A., Schneider, H., Burridge, J., Ascanio, A.K.M., Wojciechowski, T., Topp, C.N. et al. (2015) Digital imaging of root traits (DIRT): a high-throughput computing and collaboration platform for field-based root phenomics. *Plant Methods* **11**, 1–12 https://doi.org/10.1186/s13007-015-0043-0
43 Liu, S., Barrow, C.S., Hanlon, M., Lynch, J.P. and Bucksch, A. (2020) DIRT/3d : 3D phenotyping for maize (*Zea mays*) root architecture in the field 1–23. bioRxiv https://doi.org/10.1101/2020.06.30.180059
44 Delory, B.M., Baudson, C., Brostaux, Y., Lobet, G., du Jardin, P., Pagès, L. et al. (2016) archiDART: an R package for the automated computation of plant root architectural traits. *Plant Soil* **398**, 351–365 https://doi.org/10.1007/s11104-015-2673-4
45 Shahzad, Z., Kellermeier, F., Armstrong, E.M., Rogers, S., Lobet, G., Amtmann, A. et al. (2018) EZ-root-VIS: a software pipeline for the rapid analysis and visual reconstruction of root system architecture. *Plant Physiol.* **177**, 1368–1381 https://doi.org/10.1104/pp.18.00217
46 Galkovskyi, T., Mileyko, Y., Bucksch, A., Moore, B., Symonova, O., Price, C.A. et al. (2012) Gia roots: software for the high throughput analysis of plant root system architecture. *BMC Plant Biol.* **12**, 116 https://doi.org/10.1186/1471-2229-12-116
47 Seethepalli, A., Guo, H., Liu, X., Griffiths, M., Almtarfi, H., Li, Z. et al. (2020) Rhizovision crown: an integrated hardware and software platform for root crown phenotyping. *Plant Phenomics* **2020**, 1–15 https://doi.org/10.34133/2020/3074916
48 Dowd, T.G., Braun, D.M. and Sharp, R.E. (2020) Maize lateral root developmental plasticity induced by mild water stress. II: genotype-specific spatio-temporal effects on determinate development. *Plant Cell Environ.* **43**, 2409–2427 https://doi.org/10.1111/pce.13840
49 Metzner, R., Eggert, A., van Dusschoten, D., Pflugfelder, D., Gerth, S., Schurr, U. et al. (2015) Direct comparison of MRI and X-ray CT technologies for 3D imaging of root systems in soil: potential and challenges for root trait quantification. *Plant Methods* **11**, 1–11 https://doi.org/10.1186/s13007-015-0060-z
50 Garbout, A., Munkholm, L.J., Hansen, S.B., Petersen, B.M., Munk, O.L. and Pajor, R. (2012) The use of PET/CT scanning technique for 3D visualization and quantification of real-time soil/plant interactions. *Plant Soil* **352**, 113–127 https://doi.org/10.1007/s11104-011-0983-8
51 Hubeau, M. and Steppe, K. (2015) Plant-PET scans: in vivo mapping of xylem and phloem functioning. *Trends Plant Sci.* **20**, 676–685 https://doi.org/10.1016/j.tplants.2015.07.008
52 Jahnke, S., Menzel, M.I., Van Dusschoten, D., Roeb, G.W., Bühler, J., Minwuyelet, S. et al. (2009) Combined MRI-PET dissects dynamic changes in plant structures and functions. *Plant J.* **59**, 634–644 https://doi.org/10.1111/j.1365-313X.2009.03888.x
53 Moradi, A.B., Carminati, A., Vetterlein, D., Vontobel, P., Lehmann, E., Weller, U. et al. (2011) Three-dimensional visualization and quantification of water content in the rhizosphere. *New Phytol.* **192**, 653–663 https://doi.org/10.1111/j.1469-8137.2011.03826.x
54 Ahmed, M.A., Zarebanadkouki, M., Kaestner, A. and Carminati, A. (2016) Measurements of water uptake of maize roots: the key function of lateral roots. *Plant Soil* **398**, 59–77 https://doi.org/10.1007/s11104-015-2639-6
55 Rudolph, N., Esser, H.G., Carminati, A., Moradi, A.B., Hilger, A., Kardjilov, N. et al. (2012) Dynamic oxygen mapping in the root zone by fluorescence dye imaging combined with neutron radiography. *J. Soils Sediments* **12**, 63–74 https://doi.org/10.1007/s11368-011-0407-7
56 Pauli, D., Chapman, S.C., Bart, R., Topp, C.N., Lawrence-Dill, C.J., Poland, J. et al. (2016) The quest for understanding phenotypic variation via integrated approaches in the field environment. *Plant Physiol.* **172**, 622–634 doi: 10.1104/pp.16.00592

57 Guo, L., Chen, J., Cui, X., Fan, B. and Lin, H. (2013) Application of ground penetrating radar for coarse root detection and quantification: a review. *Plant Soil* **362**, 1–23 https://doi.org/10.1007/s11104-012-1455-5
58 Griffin, K.L., Ross, P.D., Sims, D.A., Luo, Y., Seemann, J.R., Fox, C.A. et al. (1996) EcoCELLs: tools for mesocosm scale measurements of gas exchange. *Plant Cell Environ.* **19**, 1210–1221 https://doi.org/10.1111/j.1365-3040.1996.tb00437.x
59 Grogan, P., Michelsen, A., Ambus, P. and Jonasson, S. (2004) Freeze-thaw regime effects on carbon and nitrogen dynamics in sub-Arctic heath tundra mesocosms. *Soil Biol. Biochem.* **36**, 641–654 https://doi.org/10.1016/j.soilbio.2003.12.007
60 Gustin, M.S., Ericksen, J.A., Schorran, D.E., Johnson, D.W., Lindberg, S.E. and Coleman, J.S. (2004) Application of controlled mesocosms for understanding mercury air-soil-plant exchange. *Environ. Sci. Technol.* **38**, 6044–6050 https://doi.org/10.1021/es0487933
61 Juvigny-Khenafou, N.P.D., Zhang, Y., Piggott, J.J., Atkinson, D., Matthaei, C.D., Van Bael, S.A. et al. (2020) Anthropogenic stressors affect fungal more than bacterial communities in decaying leaf litter: a stream mesocosm experiment. *Sci. Total Environ.* **716**, 135053 https://doi.org/10.1016/j.scitotenv.2019.135053
62 Mur, L.A.J., Prats, E., Pierre, S., Hall, M.A. and Hebelstrup, K.H. (2013) Integrating nitric oxide into salicylic acid and jasmonic acid/ ethylene plant defense pathways. *Front. Plant Sci.* **4**, 1–7 https://doi.org/10.3389/fpls.2013.00215
63 Seymour, M., Durance, I., Cosby, B.J., Ransom-Jones, E., Deiner, K., Ormerod, S.J. et al. (2018) Acidity promotes degradation of multi-species environmental DNA in lotic mesocosms. *Commun. Biol.* **1**, 1–8 https://doi.org/10.1038/s42003-017-0005-3
64 Li, M., Shao, M.R., Zeng, D., Ju, T., Kellogg, E.A. and Topp, C.N. (2020) Comprehensive 3D phenotyping reveals continuous morphological variation across genetically diverse sorghum inflorescences. *New Phytol.* **226**, 1873–1885 https://doi.org/10.1111/nph.16533
65 Li, M., Duncan, K., Topp, C.N., Chitwood, D.H. (2017) Persistent homology and the branching topologies of plants. *Am. J. Bot.* **104**, 349–353 https://doi.org/10.3732/ajb.1700046
66 Loke, M.H. (2011) Tutorial: 2-D and 3-D electrical imaging surveys. https://www.geoelectrical.com
67 Carrigan, C.R., Yang, X., LaBrecque, D.J., Larsen, D., Freeman, D., Ramirez, A.L. et al. (2013) Electrical resistance tomographic monitoring of CO2 movement in deep geologic reservoirs. *Int. J. Greenh Gas Control* **18**, 401–408 https://doi.org/10.1016/j.ijggc.2013.04.016
68 Suryanto, B., Saraireh, D., Kim, J., McCarter, W.J. and Starrs HMT, G. (2019) Imaging water ingress into concrete using electrical resistance tomography. *Int. J. Adv. Eng. Sci. Appl. Math.* **9**, 109–118 https://doi.org/10.1007/s12572-017-0190-9
69 Hisham, H., Nordiana, M.M. and Ying Jia, T. (2017) Evaluation of semanggol formation (Permian facies) using electrical resistivity tomography and seismic refraction tomography parameter. *IOP Conf. Ser. Earth Environ. Sci.* **62**, 012008 https://doi.org/10.1088/1755-1315/62/1/012008
70 Loke, M.H. and Barker, R.D. (1996) Practical techniques for 3D resistivity surveys and data inversion. *Geophys. Prospect.* **44**, 499–523 https://doi.org/10.1111/j.1365-2478.1996.tb00162.x
71 Takriff, M.S., Hamzah, A., Kamarudin, S.K. and Abdullah, J. (2009) Electrical resistance tomography investigation of gas dispersion in gas-liquid mixing in an agitated vessel. *J. Appl. Sci.* **9**, 3100–3115 https://doi.org/10.3923/jas.2009.3110.3115
72 Commer, M., Doetsch, J., Dafflon, B., Wu, Y., Daley, T.M. and Hubbard, S.S. (2016) Time-lapse 3-D electrical resistance tomography inversion for crosswell monitoring of dissolved and supercritical CO2 flow at two field sites: Escatawpa and Cranfield, Mississippi, USA. *Int. J. Greenh Gas Control* **49**, 297–311 https://doi.org/10.1016/j.ijggc.2016.03.020
73 Beff, L., Günther, T., Vandoorne, B., Couvreur, V. and Javaux, M. (2013) Three-dimensional monitoring of soil water content in a maize field using Electrical Resistivity Tomography. *Hydrol Earth Syst. Sci.* **17**, 595–609 https://doi.org/10.5194/hess-17-595-2013
74 Mary, B., Peruzzo, L., Boaga, J., Schmutz, M., Wu, Y., Hubbard, S.S. et al. (2018) Small-scale characterization of vine plant root water uptake via 3-D electrical resistivity tomography and mise-à-la-masse method. *Hydrol Earth Syst. Sci.* **22**, 5427–5444 https://doi.org/10.5194/hess-22-5427-2018
75 Mary, B., Vanella, D., Consoli, S. and Cassiani, G. (2019) Assessing the extent of citrus trees root apparatus under deficit irrigation via multi-method geo-electrical imaging. *Sci. Rep.* **9**, 1–10 https://doi.org/10.1038/s41598-019-46107-w
76 Amato, M., Basso, B., Celano, G., Bitella, G., Morelli, G. and Rossi, R. (2008) In situ detection of tree root distribution and biomass by multi-electrode resistivity imaging. *Tree Physiol.* **28**, 1441–1448 https://doi.org/10.1093/treephys/28.10.1441
77 Cassiani, G., Boaga, J., Vanella, D., Perri, M.T. and Consoli, S. (2015) Monitoring and modelling of soil-plant interactions: the joint use of ERT, sap flow and eddy covariance data to characterize the volume of an orange tree root zone. *Hydrol. Earth Syst. Sci.* **19**, 2213–2225 https://doi.org/10.5194/hess-19-2213-2015
78 Mastrocicco, M., Vignoli, G., Colombani, N. and Abu Zeid, N. (2010) Surface electrical resistivity tomography and hydrogeological characterization to constrain groundwater flow modeling in an agricultural field site near Ferrara (Italy). *Environ. Earth Sci.* **61**, 311–322 https://doi.org/10.1007/s12665-009-0344-6
79 Swileam, G.S., Shahin, R.R., Nasr, H.M. and Essa, K.S. (2019) Spatial variability assessment of Nile alluvial soils using electrical resistivity technique. *Eurasian J. Soil Sci.* **8**, 110–117 https://doi.org/10.18393/ejss.528851
80 Whalley, W.R., Binley, A., Watts, C.W., Shanahan, P., Dodd, I.C., Ober, E.S. et al. (2017) Methods to estimate changes in soil water for phenotyping root activity in the field. *Plant Soil* **415**, 407–422 https://doi.org/10.1007/s11104-016-3161-1
81 Buy, S., Le Floch, S., Tang, N., Sidiboulenouar, R., Zanca, M., Canadas, P. et al. (2018) Flip-flop method: a new t1-weighted flow-mri for plants studies. *PLoS One* **13**, 1–14 https://doi.org/10.1371/journal.pone.0194845
82 Smith, A.G., Han, E., Petersen, J., Olsen, N.A.F., Giese, C., Athmann, M. et al. (2020) Rootpainter: deep learning segmentation of biological images with corrective annotation. 1–16. bioRxiv https://doi.org/10.1101/2020.04.16.044461
83 Uga, Y., Sugimoto, K., Ogawa, S., Rane, J., Ishitani, M., Hara, N. et al. (2013) Control of root system architecture by DEEPER ROOTING 1 increases rice yield under drought conditions. *Nat. Genet.* **45**, 1097–1102 https://doi.org/10.1038/ng.2725
84 van Dusschoten, D., Metzner, R., Kochs, J., Postma, J.A., Pflugfelder, D., Bühler, J. et al. (2016) Quantitative 3D analysis of plant roots growing in soil using magnetic resonance imaging. *Plant Physiol.* **170**, 1176–1188 https://doi.org/10.1104/pp.15.01388